Modern Chemistry
2021; 9(3): 68-72
http://www.sciencepublishinggroup.com/j/mc
doi: 10.11648/j.mc.20210903.14
ISSN: 2329-1818 (Print); ISSN: 2329-180X (Online)

$BiVO_4/MnO_2$ Composite Photocatalytic Material for the Shale Gas Flowback Wastewater Treatment

Yanling Liu[1], Zhengxin Yang[1], Longjun Xu[1, *], Chenglun Liu[1, 2], Teng Zhang[1], Zao Jiang[1]

[1]State Key Laboratory of Coal Mine Disaster Dynamics and Control, Chongqing University, Chongqing, China

[2]School of Chemistry and Chemical Engineering, Chongqing University, Chongqing, China

Email address:

xulj@cqu.edu.cn (Longjun Xu), 1213019731@qq.com (Yanling Liu)

[*]Corresponding author

To cite this article:

Yanling Liu, Zhengxin Yang, Longjun Xu, Chenglun Liu, Teng Zhang, Zao Jiang. $BiVO_4/MnO_2$ Composite Photocatalytic Material for the Shale Gas Flowback Wastewater Treatment. *Modern Chemistry*. Vol. 9, No. 3, 2021, pp. 68-72. doi: 10.11648/j.mc.20210903.14

Received: September 7, 2021; **Accepted**: September 27, 2021; **Published**: September 29, 2021

Abstract: The management and disposal of the shale gas flowback wastewater is one of the greatest challenges associated with the exploration and extraction of unconventional natural gas resources. High salinity and complex chemical composition of fracturing fluids are the main limiting factors for beneficial reuse of the shale gas flowback wastewater, which has become a tough problem in the global environmental field. In this study, a composite photocatalytic oxidant of MnO_2 modified $BiVO_4$ was successfully synthesized with one-step hydrothermal method, and used to treat the shale gas flowback wastewater. The synergistic effect of photocatalysis and oxidation has made a great contribution to the removal of COD value in wastewater. When catalyst dosage was 0.6 g, the pH value was controlled to 3, and visible light exposure was 4 h, the prepared $BiVO_4/MnO_2$ exhibited the optimum photocatalytic oxidation activity, and the removal efficiency of COD could reach 65.5%, which is better than that of pure $BiVO_4$ or MnO_2. Furthermore, in this case, the COD value could be decreased from 188 mg/L to 64.9 mg/L, complying with the first-level standard limit requirements in the integrated wastewater discharge standard (GB8978-1996). Moreover, in the viewpoint of dynamics, Langmuir isothermal-like equation can better describe the relationship between COD removal efficiency and illumination time.

Keywords: Shale Gas Flowback Wastewater, Photocatalytic Technology, $BiVO_4/MnO_2$

1. Introduction

As an unconventional natural gas resource, shale gas has rich reserves and it has sparked global exploration and extraction. Hydraulic fracturing is a fundamental technology commonly used to extract natural gas from the tight shale gas reservoirs [1]. Fracturing fluids containing substances such as gelling agents, surfactants, friction reducers, corrosion and scale inhibitors have made outstanding contributions to the enhancement of shale gas recovery [2, 3]. Notwithstanding, high salinity and complex chemical composition characteristics hinder the management of shale gas flowback wastewater, which has become a tough problem in the global environmental field [4, 5]. As a result, related wastewater disposal is one of the stumbling blocks for the shale gas industry to improve overall cost effectiveness and reduce environmental impact. Reliable data shows that the COD value of shale gas flowback wastewater in Sichuan Basin is between 358 mg/L and 3477 mg/L [6]. In wastewater treatment, electrocatalytic oxidation is the most commonly used method to treat shale gas backflow wastewater. Feng [7] employed a composite RuO_2/PPy anode for degradation of organics in an electrocatalytic oxidation system with an excellent COD removal ratio of 96%. However, the electrocatalytic oxidation method has the disadvantages of high electrode cost, huge energy consumption and long reaction cycle, while the photocatalytic oxidation technology can be targeted to make up for the shortcomings of the electrochemical method [8, 9]. Photocatalytic oxidation is a mature technology for wastewater treatment, and the free radicals such as ·OH and $\cdot O_2^-$ produced in the solution can oxidize the reducible substance in the sewage [10]. Currently, common methodologies to enhance photocatalytic performance include improved morphology, rare earth

doping and semiconductor compounding. Furthermore, photocatalytic oxidation techniques have been reported mostly for simulated wastewaters with single components [11-14], such as rhodamine B, methyl orange, methylene blue and tetracycline hydrochloride etc., while reports on the degradation of COD in industrial wastewaters with high salinity are scarce. $BiVO_4$ is a chemically stable, non-toxic semiconductor photocatalyst, has great potential in the field of photocatalysis [15, 16], and MnO_2 can be used as an oxidant for the oxidation organic degradation [17]. Herein, a composite photocatalytic oxidant of MnO_2 modified $BiVO_4$ has been self-assembled, and COD was measured as a wastewater index to investigate the effect of photocatalytic technology on the treatment of shale gas flowback wastewater.

2. Experimental

2.1. Materials

$Bi(NO_3)_3{\cdot}5H_2O$, NH_4VO_3, $KMnO_4$, C_2H_5OH, HNO_3, NaOH and $C_{28}H_{31}ClN_2O_3$ (RhB) were purchased from Chengdu Kelong Chemical Ltd (Chengdu, China). The reagents used in the experiments were of analytical purity grade and used without purification.

The shale gas flowback wastewater was taken from No.4 platform of Yongchuan shale gas field of Chongqing, and the initial values of COD in the water samples were 180 ~220 mg/L and chloride ions were 4500 ~5100 mg/L.

The crystal structure and substance of the synthesized samples were analyzed by X-ray diffractometry (XRD, Shimadzu, XRD-6000, Kyoto, Japan). Furthermore, the structure and morphology of the catalyst were investigated by scanning electron microscopy (SEM, Hitachi S-4800, Hitachi, Tokyo, Japan).

2.2. Methods

A reliable hydrothermal method was used to synthesize $BiVO_4/MnO_2$. For comparison, $BiVO_4$, MnO_2 and $BiVO_4/MnO_2$ were synthesized with reference to the relevant previous practices [18].

Preparation of $BiVO_4$. 2.43 g $Bi(NO_3)_3{\cdot}5H_2O$ was dispersed in 25 mL dilute HNO_3 solution and stirred magnetically for 10 min to obtain solution A. Then add 0.58 g NH_4VO_3 to the mixed solution and stirred for 10 min, immediately adjust the pH to 6 with 2 mol/L of NaOH, $BiVO_4$ precursor solution to be prepared and stirred for another 30 min. After that, the above solution was transferred to a 100 mL Teflon-lined stainless-steel reactor and heated at 180°C for 24 h. The resulting product was then washed several times with deionized water and anhydrous ethanol and dried at 60°C overnight.

Preparation of MnO_2. 0.5136 g $KMnO_4$ was dispersed in 65 mL deionized water and stirred magnetically for 30 min. Afterwards, the above solution was transferred to a 100 mL Teflon-lined stainless-steel reactor. The following operation is the same as that of $BiVO_4$.

Preparation of $BiVO_4/MnO_2$. 0.294 g $KMnO_4$ was added to $BiVO_4$ precursor solution and stirred for 30 min under magnetic agitation. The solution was transferred to a 100 mL reactor. The following operation is the same as that of MnO_2.

Test of photocatalytic performance. The shale gas flowback wastewater was taken as the degradation raw material to test the photocatalytic performance of the prepared samples. 100 mL shale gas flowback wastewater was transferred into a 200 mL jacketed beaker maintaining the constant temperature 25°C through a water-cooling system. Before the photocatalytic procedure, dilute sulfuric acid was used to regulate pH and appropriate photocatalysts were added to the wastewater. The mixed solution was magnetically stirred for 30 min in the dark to reach the adsorption-desorption equilibrium, then a 300 W Xe lamp (λ>420 nm) was lighted on. 5 mL of the solution in the reaction vessel was separated by high-speed centrifugation every same time period (60 min). Next, the solution of COD was examined by a potassium dichromate method. The COD value can be calculated according to the formula (1), and then the COD removal efficiency η can be obtained according to the formula (2),

$$COD(O_2, \mathrm{mg}/L) = \frac{(V_0 - V_1) \times C \times 8 \times 1000}{V} \tag{1}$$

where, C represents the concentration of ammonium ferrous sulfate standard solution, V_0 represents the amount of ammonium ferrous sulfate standard titration solution consumed by blank sample, V_1 represents consumption of ammonium ferrous sulfate standard titration solution amount, V represents the volume of the sample.

$$\eta = \frac{A_0 - A_t}{A_0} \times 100\% \tag{2}$$

where, A_0 and A_t represent COD values of water samples before illumination and after illumination, respectively.

3. Results and Discussion

3.1. Crystalline Structure

Figure 1 displays the XRD patterns of $BiVO_4$, MnO_2 and $BiVO_4/MnO_2$ samples. The main diffraction peaks of $BiVO_4$ and MnO_2 samples are well coincided with the standard diffraction of $BiVO_4$ with monoclinic scheelite structure (JCPDS Card No. 14-0688) and MnO_2 with birnessite-type (JCPDS Card No. 80-1098). Meanwhile, it was observed that facets detected (001), (002), (111) and (311) belong to the MnO_2. Besides, these characteristic diffraction peaks of $BiVO_4$ are found in the XRD pattern of $BiVO_4/MnO_2$, indicating the facets detected of (-121), (-130), (040), (011), (110), (161), (042) and (240) belong to the $BiVO_4$. Nevertheless, only one diffraction peak attributed to the (051) plane of MnO_2 can be found at 42.4°, presumably due to the low content and high dispersion in the composite samples.

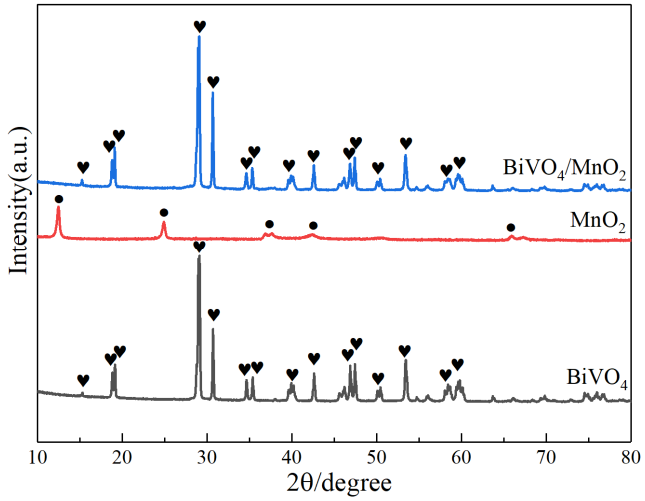

Figure 1. *XRD patterns of $BiVO_4$, MnO_2 and $BiVO_4/MnO_2$.*

Figure 2 displays the SEM patterns of $BiVO_4$ and $BiVO_4/MnO_2$ samples. It can be found that $BiVO_4$ had a smooth flaky dumbbell shape in Figures 2a and 2b. It can also be found that MnO_2 with nanoparticle morphology is uniformly dispersed on the surface of nanoblock $BiVO_4$ in Figures 2c and 2d, increasing the specific surface area and providing more effective contact area for the reaction of pollutants with the catalyst.

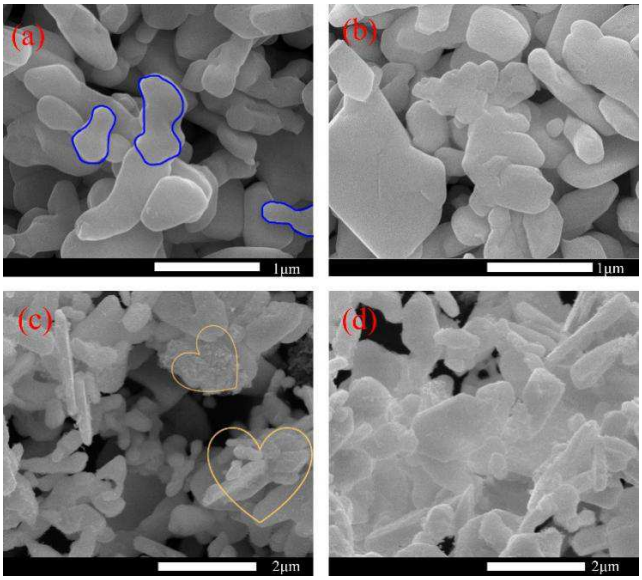

Figure 2. *SEM patterns of $BiVO_4$ and $BiVO_4/MnO_2$.*

3.2. Effect of Different Samples on COD Degradation

At the start of the experiment, 100 mL shale gas flowback wastewater was placed in a 200 mL reactor, equipped with external recirculating cooling water. Next, prudently drop 1 mol/L sulfuric acid to adjust the pH to 3. Besides, 0.2 g $BiVO_4$, MnO_2 and $BiVO_4/MnO_2$ were respectively added to 200 mL jacketed beaker under magnetic agitation. The mixed solution was stirred in the dark for 30 min to achieve adsorption equilibrium. Table 1 shows the variation trend of COD after 4 h of photocatalysis under the xenon lamp system.

Table 1. *Degradation wastewater data record sheet of each material.*

number	samples	initial COD	eventual COD
1	blank	211.6 mg/L	210.6 mg/L
2	$BiVO_4$	180.8 mg/L	162.0 mg/L
3	MnO_2	209.4 mg/L	120.1 mg/L
4	$BiVO_4$/ MnO_2	221.8 mg/L	103.1 mg/L

Under similar conditions, the influence of different samples on the COD degradation efficiency was studied. As shown in Figure 3, the COD removal efficiency in all samples increases with the extension of the illumination time. The degradation efficiency of COD has been calculated, Blank, $BiVO_4$, MnO_2 and $BiVO_4/MnO_2$ are 0.4%, 10.4%, 42.4% and 53.5%, respectively. It can be observed that the COD removal efficiency of $BiVO_4/MnO_2$ has been greatly improved compared to $BiVO_4$ from 10.4% to 53.5%. The possible reasons are as follows. First, an addition of appropriate amount of nanoparticle MnO_2 increases the pore size and specific surface area of the composite [18], and this makes more contact area between pollutants and photocatalysts, hence the photocatalytic activity enhances. Second, when doping MnO_2 into $BiVO_4$ nanoblock, $BiVO_4/MnO_2$ is expected to increase the opportunities of more photogenerated electron–hole pairs. Under simulated visible light illumination, the dissolved oxygen captures photogenerated electrons in solution, and the photogenerated holes oxidize OH^- to form $O_2\cdot$ and ·OH, respectively. In the meanwhile, these strong free radicals promote the removal of organic matter in shale gas flowback wastewater. Third, the highest oxidation activity of MnO_2 exists in an appropriate pH solution. Furthermore, the synergistic effect of $BiVO_4$ and MnO_2 can realize the efficient treatment of wastewater. It is clear that $BiVO_4/MnO_2$ has the best photocatalytic activity among all the samples. In consequence, $BiVO_4/MnO_2$ will be used to further explore the treatment effect of photocatalytic oxidation technology on shale gas flowback wastewater in the following experiment.

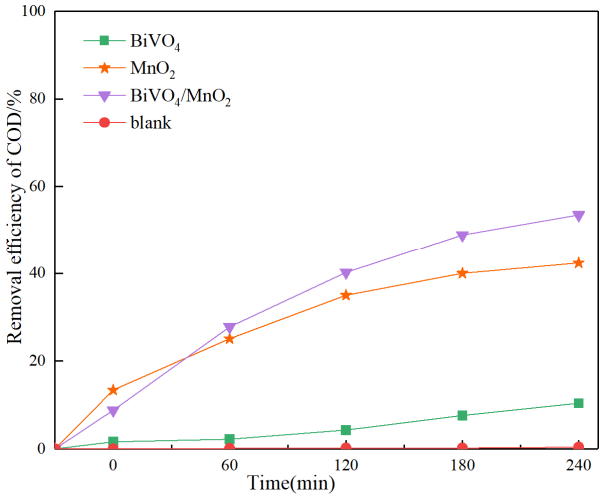

Figure 3. *The COD degradation efficiency varies with the illumination time.*

3.3. Effect of $BiVO_4/MnO_2$ Dosage on COD Degradation

On the basis of 3.2, different amounts of $BiVO_4/MnO_2$ (0.2 g, 0.4 g and 0.6 g) are added to the shale gas flowback

wastewater to investigate the relation between the photocatalytic activity and the $BiVO_4/MnO_2$ addition. The initial COD value of wastewater was188 mg/L, and the pH of the solution was controlled to 3. In this case, the photocatalytic activity of 0.6 g $BiVO_4/MnO_2$ is slightly high compared with 0.2 g and 0.4 g $BiVO_4/MnO_2$, namely the degradation efficiency increases to 65.5%. It is seen that the COD degradation curve gradually flattens with the increasing of illumination time in Figure 4. This may be attributed to the following two points. Firstly, as the dosage of photocatalyst increases, more precursors of catalyst active sites are produced. This leads to the oxidation of pollutants in wastewater by more strong oxidation free radicals, which transform macromolecular organic matter into small molecules such as CO_2 and H_2O, resulting in improving the catalytic removal efficiency of COD. Secondly, as the reaction proceeds, the easily degradable organic matter in the wastewater is consumed. In this case, the remaining macromolecular organic matter hinders the reaction process, and the degradation process becomes slower and slower. In conclusion, the addition amount of $BiVO_4/MnO_2$ in the following experiment is set as 0.6 g.

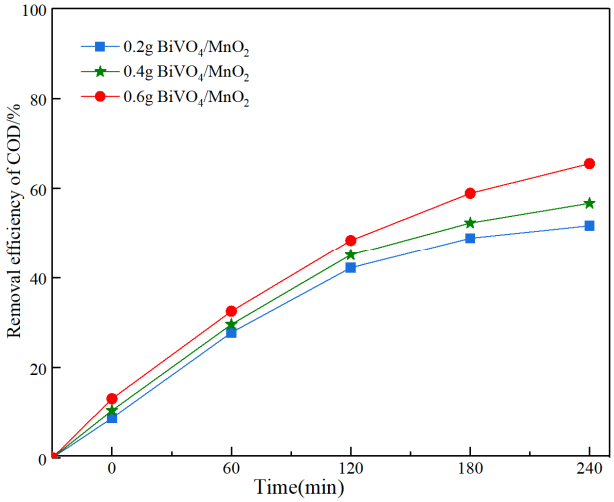

Figure 4. *The COD removal efficiency of $BiVO_4$/ MnO_2 with different quality varies with the illumination time.*

It can be observed in Figure 4 that the increment of COD removal efficiency decreases as the extension of the illumination time. Moreover, the variation relationship between COD removal efficiency and illumination time is similar to that between adsorption capacity and pressure in Langmuir monolayer adsorption equation. Therefore, it is assumed that the quantitative relationship between COD removal efficiency η and illumination time t can be depicted by a similar equation to Langmuir isothermal equation, as shown in the following formulas (3):

$$\eta = \frac{abt}{1+bt} \tag{3}$$

$$\text{or } \frac{t}{\eta} = \frac{1}{ab} + \frac{t}{a} \tag{4}$$

where, *a* and *b* are constants.

All data in Figure 4 are linearly fitted according to formula (4), the constant values and correlation coefficient of the linear relation obtained are listed in Table 2.

Table 2. *Constant a, b and correlation coefficient.*

$BiVO_4/MnO_2$ dosage(g)	*a*	*b*	*r*
0.2	75.99	0.36	0.986
0.4	79.74	0.34	0.976
0.6	118.06	0.20	0.991

As can be seen from Table 2, equation (4) can better describe the relationship between COD removal efficiency η and illumination time *t*. Constant *a* reaches the maximum value when the $BiVO_4/MnO_2$ dosage is 0.6 g, indicating that the COD removal efficiency is the highest when the catalyst dosage is 0.6 g, which is agreement with the results shown in Figure 4. In the meantime, constant *b* reaches the maximum value when the $BiVO_4/MnO_2$ dosage is 0.2 g, indicating that reaction ratio is the highest at this time.

3.4. Effect of pH on COD Degradation

Based on section 3.3, under the similar conditions, the influence of different pH values (pH=1, 3, 5) on COD degradation was investigated. The initial COD value of wastewater was 188 mg/L, catalyst dosage was 0.6 g. According to Figure 5, it can be clearly seen that the COD treatment efficiency is 49.9% when pH=1, the COD removal efficiency is 54.7% when pH=5. While, the degradation efficiency reaches 65.5% at pH=3, showing good photocatalytic activity. Moreover, the COD value decreased from 188 mg/L to 64.9 mg/L, meeting the first-level standard limit requirement of the integrated wastewater discharge standard (GB8978-1996). Otherwise, it could be observed that the ultra-low pH solution inhibits the photocatalytic activity of the sample. Thus, $BiVO_4/MnO_2$ was suppressed at pH=1. It implies that too many hydrogen ions in the water means fewer hydroxide ions. Consequently, fewer holes oxidize the OH^- to form the ·OH which plays a major role in the photocatalytic process. Thus, the removal of pollutants from wastewater is reduced.

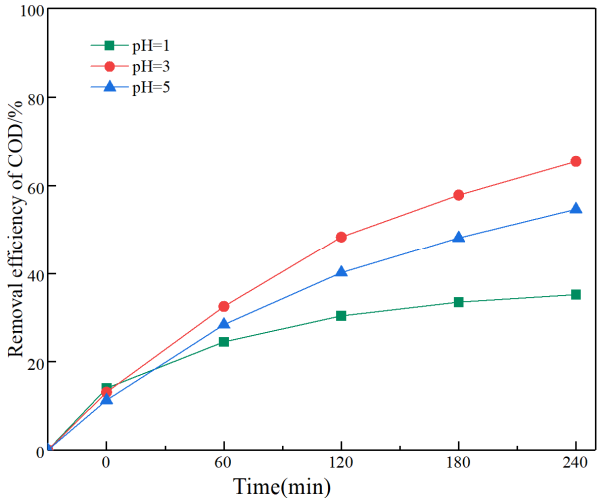

Figure 5. *Removal efficiency of COD with time at different pH values.*

Depicted relationship between t/η and t by use of the Langmuir isothermal-like equation (4), each data in Figure 5 is linearly fitted, the constant values and correlation coefficient of the linear relation obtained are listed in Table 3.

Table 3. *Constant a, b and correlation coefficient.*

the pH of the solution	*a*	*b*	*r*
1	32.03	0.50	0.998
3	118.06	0.20	0.991
5	88.34	0.24	0.999

As can be seen from Table 3, equation (4) can better describe the relationship between COD removal efficiency η and illumination time t. Constant a reaches maximum value at the solution pH=3. It means that the COD removal efficiency is the highest at this point, which is consistent with the results shown in Figure 5. In addition, the constant b is maximum at the solution pH=1, suggesting that the reaction ratio is the highest at this time.

4. Conclusion

In summary, a binary photocatalyst $BiVO_4/MnO_2$ was successfully synthesized with one-step hydrothermal method, and used to treat the shale gas flowback wastewater. When catalyst dosage was 0.6 g, the pH value was controlled to 3, and exposed to visible light for 4 h, the prepared $BiVO_4/MnO_2$ exhibited the optimum activity, and the removal efficiency of COD could reach 65.5%, which is better than that of pure $BiVO_4$ and MnO_2. Furthermore, in this case, the COD value could be decreased from 188 mg/L to 64.9 mg/L, complying with the first-level standard limit requirements in the integrated wastewater discharge standard (GB8978-1996). Langmuir isothermal-like equation can better describe the relationship between COD removal efficiency and illumination time. The excellent photocatalytic activity of $BiVO_4/MnO_2$ can be attributed to the synergistic effect of photocatalysis and oxidation, the increase of specific surface area and more active substances. In addition, the photocatalytic oxidation process can be coupled with other processes in order to obtain better treatment effect for shale gas flowback wastewater.

Acknowledgements

This work was supported by the National Natural Science Foundation of China (52174157) and Innovative Talents Training Program for Chongqing Primary and Secondary School Students (CY200148). Thank Zhou Jinqi from Yucai Middle School for participating in part of the experiment.

References

[1] Estrada J M, Bhamidimarri R. A review of the issues and treatment options for wastewater from shale gas extraction by hydraulic fracturing [J]. Fuel. 2016, 182: 292-303.

[2] WEI Z, Qianning T, Haihua W. Research of the pollution on Groundwater by Shale Gas Exploitation and Progress in Countermeasure Study [J]. 2015, (04): 52-56.

[3] Barati R, Liang J-T. A review of fracturing fluid systems used for hydraulic fracturing of oil and gas wells [J]. Journal of Applied Polymer Science. 2014, 131 (16).

[4] Gregory K B, Vidic R D, Dzombak D A. Water management challenges associated with the production of shale gas by hydraulic fracturing [J]. Elements. 2011, 7 (3): 181-186.

[5] Chang H, Li T, Liu Betc. Potential and implemented membrane-based technologies for the treatment and reuse of flowback and produced water from shale gas and oil plays: A review [J]. Desalination. 2019, 455: 34-57.

[6] Chang H Q, Li T, Liu B C etc. Potential and implemented membrane-based technologies for the treatment and reuse of flowback and produced water from shale gas and oil plays: A review [J]. Desalination. 2019, 455: 34-57.

[7] Qi F, Fang H, Derong L etc. Preparation and Electrocatalysis Performance of Composite RuO_2-PPy Electrode [J]. 2018, 47 (12): 105-112.

[8] Buzzetti L, Crisenza G E M, Melchiorre P. Mechanistic Studies in Photocatalysis [J]. Angewandte Chemie-International Edition. 2019, 58 (12): 3730-3747.

[9] Ibhadon A O, Fitzpatrick P. Heterogeneous Photocatalysis: Recent Advances and Applications [J]. Catalysts. 2013, 3 (1): 189-218.

[10] Dongmei L, Wencong L, Yicong L etc. Room-temperature precipitation synthesis and photocatalysis of Bi_5O_7I/g-C_3N_4 Z-scheme heterojunction [J]. 1-9.

[11] Xiang W. Preparation and Characterization of $BiVO_4/MnO_2$ Composite magnetic photocatalytic-oxidant [D]: Chongqing University 2019.

[12] Jiabao Z. Study on degradation of dye wastewater by MIL-100(Fe) based composite [D]: XI'AN University of Science and Technology 2020.

[13] Yan L, Shuang S, Linxi S etc. Sonochemical fabrication and photocatalytic properties of Au-modified nano ZnO [J]. 1-9.

[14] Jun C, Yuan L, Guoshu W etc. Synthesis and photocatalytic performance of urchin-like TiO_2-ZnO microspheres [J]. 1-14.

[15] Chi Hieu N, Fu C-C, Juang R-S. Degradation of methylene blue and methyl orange by palladium-doped TiO_2 photocatalysis for water reuse: Efficiency and degradation pathways [J]. Journal of Cleaner Production. 2018, 202: 413-427.

[16] Wang J, Liu C, Yang S etc. Fabrication of a ternary heterostructure $BiVO_4$ quantum dots/C-60/g-C_3N_4 photocatalyst with enhanced photocatalytic activity [J]. Journal of Physics and Chemistry of Solids. 2020, 136.

[17] Rao P M, Cai L, Liu C etc. Simultaneously efficient light absorption and charge separation in $WO_3/BiVO_4$ core/shell nanowire photoanode for photoelectrochemical water oxidation [J]. Nano Letters. 2014, 14 (2): 1099-1105.

[18] Miao L, Wang J, Zhang P. Review on manganese dioxide for catalytic oxidation of airborne formaldehyde [J]. Applied Surface Science. 2019, 466: 441-453.